2 LITERATURE REVIEW

2.1 Iron Minerals:

Minerals containing iron ore are mainly of three types, oxides, hydroxides and carbonates.

A few of them are listed below.

Oxides	Hydroxides	Carbonates
FeO Wustite	α FeO.OH, Goethite	$FeCO_3$ Siderite
Fe_3O_4 Magnetite	γ FeO(OH) Lepidocrosite	
Fe_2O_3 Hematite	α $FeO(OH).nH_2O$ Limonite	

2.1.1 Thermal behaviour of iron oxides[17]

Wustite (FeO):

It is an oxide of bivalent iron and is rarely encountered in nature.It oxidises relatively at lower temperature in the range of 275-325^{0}C to higher oxide hematite. This results in weight gain.

Magnetite (Fe_3O_4):

It consists of one bivalent iron and two trivalent iron ions in spinel structure. On heating, the bivalent iron oxidizes which appears on thermal curve as an exothermic effect accompanied by a weight gain in the temperature range of 350-400^{0}C. The resultant Fe_2O_3 passes through polymorphous transformation in to α-form. This causes a slight endothermic effect to appear on the DTA curve between 650-800^{0}C.

Hematite(Fe_2O_3):

It is an oxide of trivalent iron which exists in two form viz α-Fe_2O_3 and γ-Fe_2O_3.They don't show any thermal transformation upto 1000°C. If any thermal effect appears on thermal curves, it is due to associated impurities.

2.1.2 Thermal behaviour of iron hydroxides:

Goethite [α FeO.(OH)]:

Presence of goethite in iron ore is common and reported by many investigators[10,18,19]. On heating this compound decomposes with absorption of heat[20]

$$2\{\alpha\ FeO.(OH)\} \rightarrow \alpha\ Fe_2O_3 + H_2O\uparrow$$

A well crystallized sample will give a single large endothermic peak at about 380°C. According to Topar's data the thermal dehydration effect of goethite is situated between 250°C to 360°C. The presence of impurity causes a shift in temperature of thermal effect. The peak temperature is lowered with increasing Al^{+++} contents, incorporated into the goethite structure, where they substitute a trivalent ion of iron.[21] The decrease in temperature is generally around 20 to 30°C. Akiyama el al [10,14] reports the decomposition of Australian iron ore containing goethite and kaolinite and indicate that the decomposition peak of goethite occurs at around 300°C in DSC plot. Figure 2.1 indicates their observation.

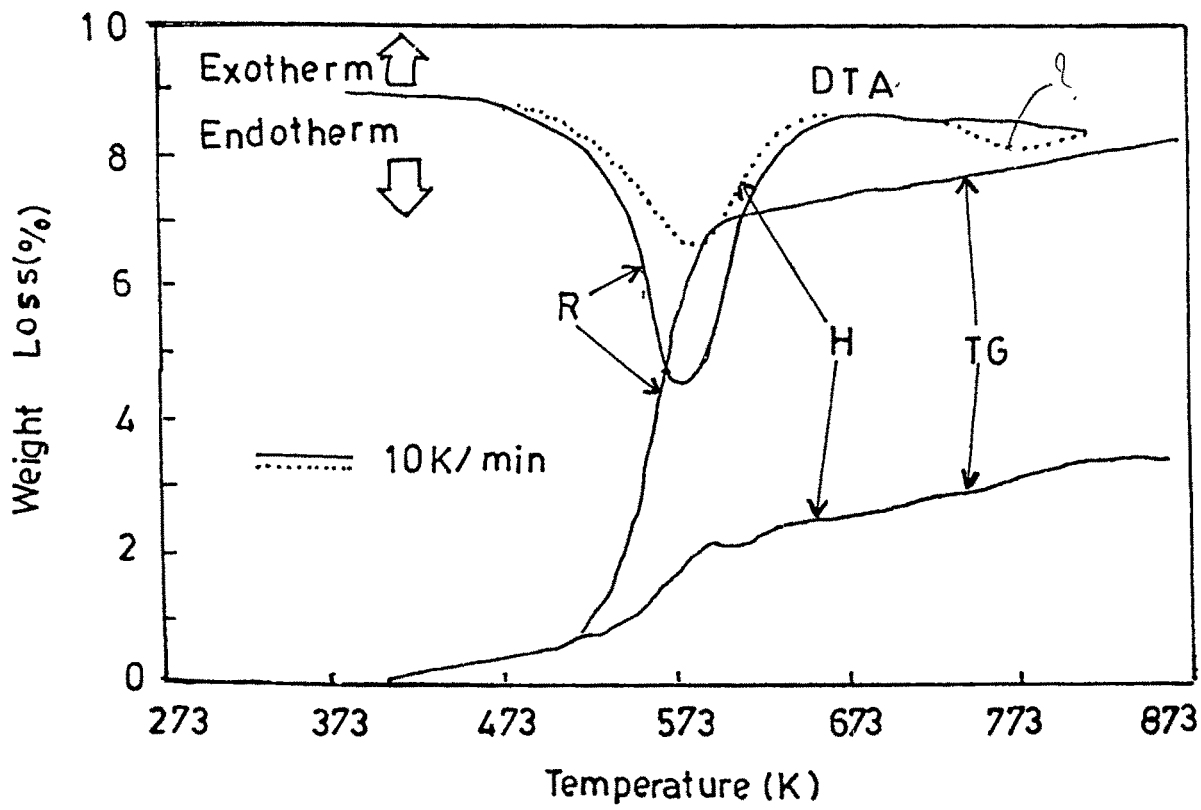

Fig. 2.1 Decomposition of Australian iron ore
(R, H : Different ores)

Lepidocrocite (γ FeO.OH):

Chemical formula for this mineral is identical to that of goethite but analytical determination shows that it contains lesser impurities than goethite. On heating both minerals behave similar for the elimination of OH group but DTA curves are different for them. In case of lepidocrocite, after the endothermic effect caused by removal of OH group an exothermic effect appears on DTA curve between 400-500^{0}C as a result of polymorphous transformation of γ Fe_2O_3 to α Fe_2O_3.

Limonite:(α- FeO(OH).nH_2O)

When water content is higher, the mineral is called limonite. According to Topar's data the thermal dehydration effect of limonite appears between 350 - 400^{0}C. Thermal decomposition curves for these hydroxides is given in figure 2.2.

Siderite: ($FeCO_3$)

Decomposition of siderite takes place by absorption of heat around 450–600^{0}C having its maximum effect at around 580^{0}C

2.2 Thermal Behaviour of Gangue

The iron ores are classified according to the gangue with which they are associated as [1, 22]

1. Siliceous ores 2. Calcareous ores 3. Aluminous ores etc.

The association of quartz, kaolinite and feldspar are also reported to be present as gangue in iron ores[23]. The kaolinite is a clay mineral with composition

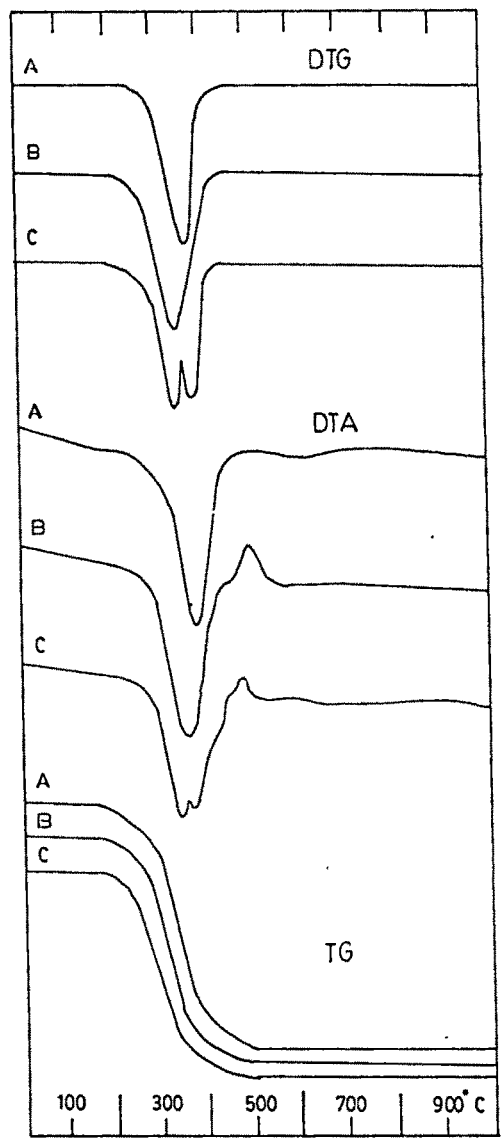

Fig. 2.2 Thermal curves for iron hydroxides:
A,Goethite-limonite; B,lepidocrocite; C,limonite-lepidocrocite.
(Ref. No: 17)

$Al_2Si_2O_5(OH)_4$ and has SiO_2-46.54%, Al_2O_3-39.50%, and H_2O- 13.95%. The mineral decomposes with removal of hydroxyls in temperature range of 450-700^{0}C depending on the type of kaolinite. Figure 2.1 indicates the decomposition of Australian iron ore containing goethite and kaolinite reported by Akiyama.[10,14] The first endothermic peak indicate decomposition of goethite and later small hump the kaolinite decomposition. Figure 2.3 depicts the decomposition peak of other clay minerals.[24]

2.3 Pellets and Pelletization:

Iron ore is the basic input material for iron making. The maximum size of the ore for Indian blast furnace is 50 - 55 mm and minimum is 10 mm.[1] Large scale iron ore mining and subsequent crushing, sieving and other processes results in generation of fines that do not find any use in iron making processes, thus leading to accumulation and environmental problems. Pelletization[25] is one of the known methods to convert these fine particles to uniform size spherical pellets. Lack of supply of high quality lump ore, better porosity and reducibility of pellet increase the acceptability of pellet as charge, specially in gas based direct reduction process. In pelletization the fine powder is rolled in to spherical balls by using disc or drum pelletitzer with addition of binder and water. Literature is available on the mechanism of ball formation and growth kinetics of green balls[26]. These green balls are subsequently dried and fired at higher temperature to attain strength by diffusion bonding or by slag/ liquid phase sintering.

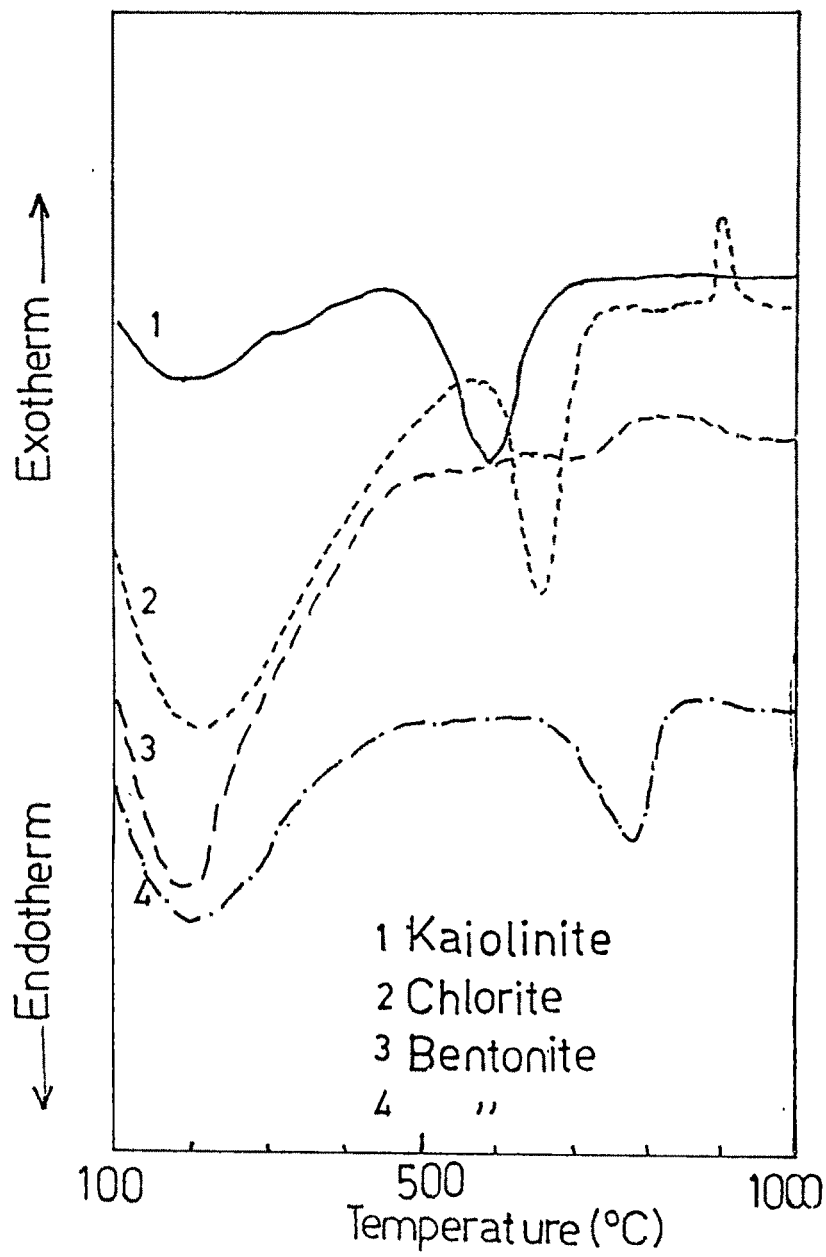

Fig. 2.3 Differential thermal analysis of clays (Ref. No. 24)

2.4 Phase Change and Mineral Assimilation on Heating Iron Ores:

The last step of pellet formation is the thermal induration of dried pellet. The induration imparts such characteristics to the pellet, which are needed for their transportation and subsequent metallurgical treatment.

During firing, two phenomena occur:

1. Change in the crystalline structure either by crystal transformation and growth (e.g. magnetite →oxidise→hematite→growth of hematite crystals) or only by crystal growth[5,15].
2. The reaction between slag forming constituents which are either present as gangue in ore or added as additives during ball formation [27,28].

Iron ores are basically treated as Fe_2O_3-Al_2O_3-CaO-SiO_2 system[29]. Many investigations are reported on the mineral formation on heating iron ore containing CaO, SiO_2 and Al_2O_3. The product minerals reported are fayalite, calcium silicate, calcium olivine, mono calcium ferrite and di-calcium ferrite [25,30]. It is reported that reaction between quartz and hematite hardly takes place on heating. Similarly no reaction would be noticed between CaO and SiO_2 even up to 1300°C for 30 min in air. However in the field of cement industry. it is known that caustic lime reacts with clay and silica and that calcium-silicate, such as $CaO.SiO_2$ is formed by heating it at about 800°C. It is also known that rate of reaction between lime and clays is much greater than that between lime and silica. Kunni et al studied the minerals of self fluxing pellets for various basicities and reported that if the basicity is lower than 0.5

most of the SiO_2 constituents react with CaO constituents to form $CaO.SiO_2$ but if the basicity is higher than 0.5, along with $CaO.SiO_2$, calcium ferrite is formed. Formation of these compounds also depends on the rate of heating. In Fe_2O_3-CaO system reaction takes place more readily than in other systems. Formation of $CaO.Fe_2O_3$ was reported by Matsuno and Kunni, in the temperature range of 950-1000^{0}C.

Matsuno and Harda [23] however indicate the subsequent dissolution of silica in ferrite melt forming, silicate melt and iron oxide. Wynnyckyj [15] reports that nature of melt formed depends on oxygen potential of the system. In case of higher oxygen potential calcium ferrite melt is formed but at lower oxygen potential, it forms silicate melt. Trivalent iron ion does not form silicate[15]. Kasai and Saito[31] studied the melt formation of several ores using thermal analysis. Shape and sequence of peaks depends on content of SiO_2, CaO and Al_2O_3. Broader peaks due to prolonged melting of calcium ferrite were also reported.

Melt formation during induration affects the pore formation and sintering process of iron ore. It is reported that iron ore sintering is a liquid phase sintering process except in case of very pure oxides. The literature on sintering of ceramics and powder metals show that pore formation in solid state sintering and in liquid phase sintering is quite different. Yang and Standish[7] studied the mechanism of pore formation. They observed that quite a number of factors have an influence on pore formation and resultant porosity. Larger initial pore gives higher average pore size and the pore tend to be more open with higher porosity.

The chemical composition of raw mix effects porosity. Porosity decreased with increasing basicity or the amount of SiO_2 due to formation of melts.[28] The porosity increased with increase in amount of MgO due to decreased amount of melt. In solid phase sintering pores are formed at inter-particle voids but in liquid phase sintering, some pores form at inter particle voids and some form at the site of local melting where the liquid flowed away[7]. In some other systems, pore were not formed at the site of melting as the liquid drew the surrounding particles together. The porosity of iron oxide compacts decreases significantly with increasing firing temperature and time in certain range.[9] Many researchers found that porosity of pellet decreased with increasing firing temperature due to increased amount of melt which caused shrinkage. Porosity of the pellet affects the mechanical and thermal properties of the pellets. Relationship between crushing strength and porosity of pellet as, reported by Wynnyckyj and Fahidy, is indicated in figure 2.4.

Porosity dependent effective thermal conductivity was examined at 1000^0C for coke samples by Kasai et al.[32] The results are indicated in figure 2.5 The effective thermal conductivity decreases with increase in porosity.

2.5 Sintering(Densification) of Pellets:

Many investigation are reported on sintering kinetics and densification of iron ore pellets [33,34,35]. Various parameters were used to represent the rate of densification. A concept for determining sintering mechanism was for the first time quantified by Kuczynski. He recognized viscous / plastic flows, vapour transport,

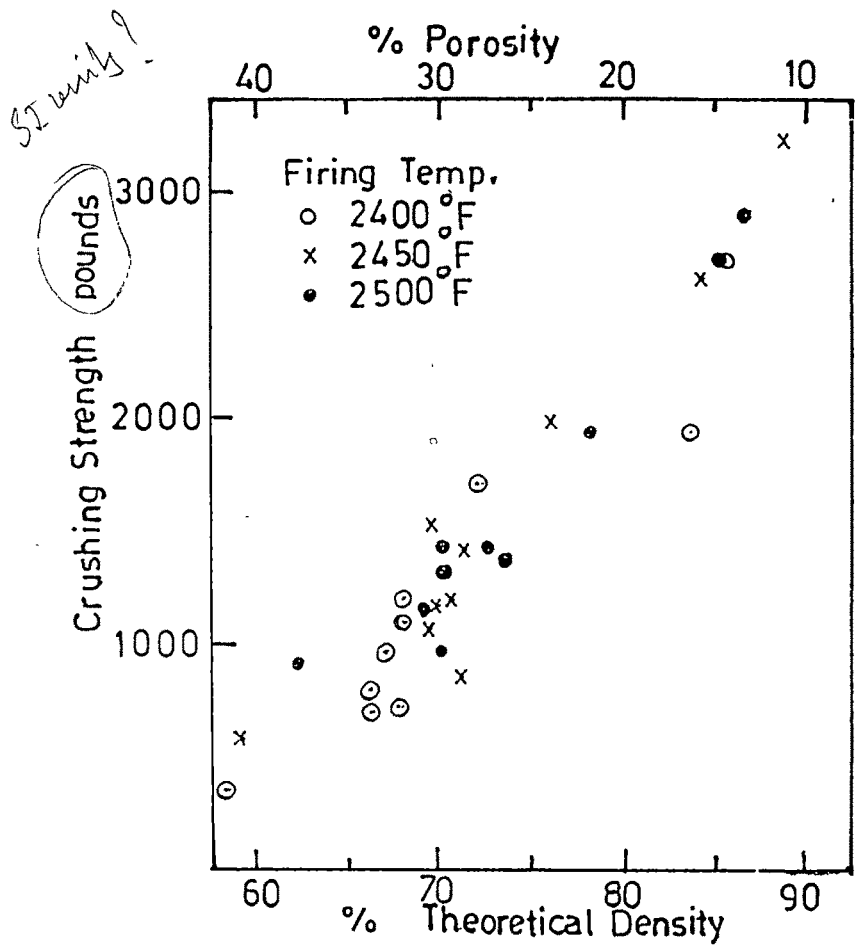

Fig. 2.4 Effect of porosity on crushing strength of pellet (Ref. No. 6)

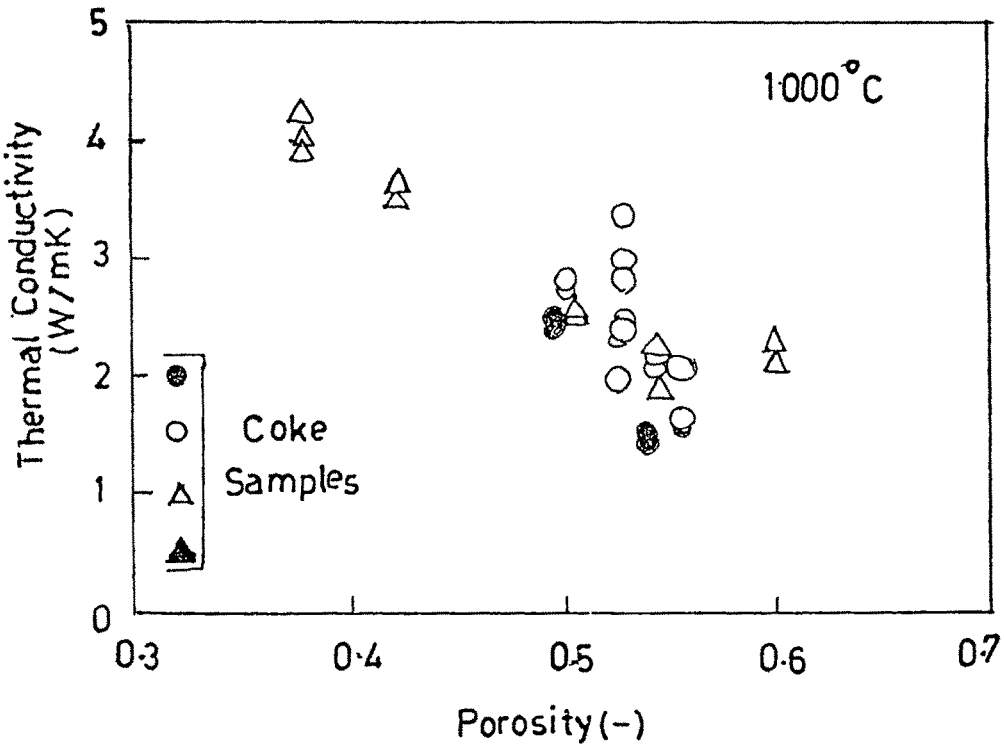

Fig 2.5 Effect of porosity on thermal conductivity of coke.
(Ref. No. 32)

lattice diffusion and surface diffusion as the possible mechanisms. The general form of equation [36]

$$(d/a)^{p} = F(T)\ t\ a^{(q-p)} \qquad \text{(2.1)}$$

Where 'd' is radius of disc of contact of two particles and 'a' is particle radius, 't' time, p and q are constants. In this equation the exponent 'p' is representative of the operative mechanism. In the plot between **log (d/a) verses log t**, the inverse slope gives the values of exponent 'p'.

The change in approach was first suggested by Kingery and Berg and then with some modification by Coble, Kuczynski and Ichinose. It was shown that inspite of complex geometries of the particles and pores in a compact, the shrinkage in the compact (instead of neck size) can be incorporated in an equation for isothermal sintering. The familinar form for this equation is like

$$\Delta L/L_0 = F(T)\ t^{p} \qquad \text{(2.2)}$$

Coble working with pressed Fe_2O_3 showed that initial sintering takes place by a bulk diffusion mechanism[33], The diffusion of Fe^{+++} being rate controlling. Kuczynski et al worked with impure Fe_2O_3 and reported two activation energy values 418.6 kJ/mol and 87.9 kJ/mol below and above 900^0C.

Yusfin and Co-workers[4] studied the mechanism of strengthening of hematite by sintering briquettes using shrinkage as criterion. The mechanism[32] reported was diffusional viscous flow with activation energy 58.6 kJ/mol .

Ross and Ohno studied the effect of heating rate, maximum temperature, particle size and soaking time upon strength and % shrinkage of hematite and magnetite briquettes. It was shown that shrinkage always began during heating at temperature below that necessary to cause sintering. Shrinkage was more pronounced with hematite than with magnetite, though magnetite is much easier to agglomerate. Mishra and Sen[33] used dilatometer and applied equation, consisting porosity change with time to interpret their result.

$$1/P^b - 1/Po^b = Kt \qquad \text{(2.3)}$$

'P' is porosity ,' b ' is constant , 'K' constant containing diffusion coefficient.

$$Po=\beta((Lo-L_T)/ L_0)^3 \qquad \text{(2.4)}$$

and

$$P=\beta((L-L_T)/ L_0)^3 \qquad \text{(2.5)}$$

where L_T is the true length and L_o the initial length and 'β' a constant

They studied the effect of alumina addition in iron ore and it was found that the addition of it decreases the percentage (%) shrinkage.

German and Muniar have related the neck size to the specific surface area. Following equation using neck size and specific surface area was reported.

$$\Delta S/So = K (\beta t)^{q/N} \qquad \text{(2.6)}$$

'K'. 'q', 'β' are constants and ΔS/So is relative change in specific surface area.

Wynnnyckyj and Fahidy[6] used change in volume as a criterion to define densification and introduced a term called 'impingement' factor and further analysed the process as other diffusion controlled processes. The model was applicable to first and intermediate stages of sintering. The much detailed review on sintering process is reported by Thummler and Thomma [35]. They indicate that the densification is better represented by parameter other than directly measured shrinkage i.e $\Delta L/Lo$ or $\Delta V/Vo$.

The dimensionless term with standardized maximum value of '1' at theoritical density is indicated to explain the process. The parameters are,

(Lo-Lsint) / (Lo-Ltheo) or (Vo-Vsint) / (Vo-Vtheo.)

In the present work parameter as volume ratio is used to explain our results.

2.6 Reaction Kinetics:

The kinetic parameters of a reaction are usually determined by two approaches.

1. Isothermal kinetics
2. Non-isothermal kinetics

Isothermal determination of kinetic parameters has many limitations. An isothermal process is an abstraction[37]. Strictly speaking no reaction takes place isothermally because all reactions are accompanied by heat change. More over time lapse occur for specimen to attain a thermal equilibrium and it is not possible without significant pre-reaction. Yang and Standish[7] made an attempt to see how soon the sample could be heated up to the furnace temperature and observed that

the temperature at the centre of the sample reached close to set furnace temperature of (1265°C) in 3.5 min. Seaton[16] also made similar observation.

Non-isothermal kinetic studies are carried out by allowing a reaction to take place progressively using a well-defined temperature-time sequence. This technique overcomes several limitations of isothermal technique and widely accepted. Ray et al applied this technique to explain decomposition kinetics of lime-stone and for gaseous and solid state reduction of Fe_2O_3[37-40].

2.6.1 Reaction rate under non-isothermal conditions.

The theoretical treatment of kinetic data obtained under rising temperature tests is done on combination of three basic equations[37].

The first, kinetic law

$$dx/dt = K(T)\, f(x).\varphi(x,T) \qquad \text{(2.7)}$$

where K(T) = Temperature dependence of specific rate constant, 'φ' and 'f' are functions, t- time and T- temperature.

Generally the $\varphi(x,T)$ is assumed to be unity which modifies the equation to

$$dx/dt = K(T)\, f(x) \qquad \text{(2.8)}$$

The second equation describes temperature dependence of the rate constant.

$$K = A.\, e^{-(E/RT)} \qquad \text{(2.9)}$$

The third equation describes the variation of temperature T, with time and for linear heating rate.

$$T = To + B\,t \qquad \text{_____ (2.10)}$$

Where 'To' is initial temperature, 'B' the heating rate and 'T' the temperature at time 't'

Combining the equations (2.8) and (2.9)

$$dx/dt = A\,e^{-(E/RT)}.\,f(x) \qquad \text{_____ (2.11)}$$

Differentiating equation 2.10

$$dT = B.dt \qquad \text{_____ (2.12)}$$

Subsituting in equation 2.11

$$dx/dT = (A/B)\,e^{-(E/RT)}\,f(x) \qquad \text{_____ (2.13)}$$

or

$$dx/f(x) = (A/B)\,e^{-(E/RT)}\,dT \qquad \text{_____ (2.14)}$$

The equation (2.14) is the basic equation in non isothermal kinetic analysis.

2.6.2 Integration of equation for function f(x) of form (1-x) ^{n}

For the simple form of function $f(x) = (1-x)^n$ the basic equation modifies to

$$dx/(1-x)^n = (A/B)\,e^{-(E/RT)}\,dT \qquad \text{_____ (2.15)}$$

Integrating

$$\int_{x_1}^{x_2} dx/(1-x)^n = (A/B)\int_{T_1}^{T_2} e^{-(E/RT)}\, dT \qquad \text{(2.16)}$$

$$= (ART^2/BE)\, e^{-(E/RT)}\, [\, 1-(2RT/E)\,] \qquad \text{(2.17)}$$

If n= 1

$$-\ln(1-x) = (ART^2/BE)\, e^{-(E/RT)}\, [\, 1-(2RT/E)] \qquad \text{(2.18)}$$

$$\ln[-\ln(1-x)] = \text{Constant}-(E/RT) \qquad \text{(2.19)}$$

This equation could be used to evaluate the value of activation energy at different fractions of reaction by plotting the L.H.S. function Vs 1/T.The change in activation energy value will indicate the change in reaction or in its mechanism.

2.6.3 Second derivative of equation:[41]

Several approaches to use the second derivative of basic equation

$$dx/dT = (A/B)\, e^{-(E/RT)}\, (1-x)^n \qquad \text{(2.15)}$$

Differentiating equation (2.15)

$$d^2x/dT^2 = (A/B)e^{-(E/RT)}(E/RT^2)(1-x)^n - (A/B)e^{-(E/RT)} n\,(dx/dT)/(1-x)^{(n-1)} \qquad \text{(2.20)}$$

$$d^2x/dT^2 = (A/B)\, e^{-(E/RT)}\, (1-x)^n\, [\, E/RT^2 - n\,(dx/dT)/(1-x)\,] \qquad \text{(2.21)}$$

$$= dx/dT\, [\, E/RT^2 - n\,(dx/dT)/(1-x)\,] \qquad \text{(2.22)}$$

At the inflexion point of a TG curve or at peak of DTA/DSC the second derivative is zero. Thus,

$$[\, E/RT_{max}^2 - (dx/dT)_{max}\, n/(1-X_{max})\,] = 0 \qquad \text{(2.23)}$$

$$(dx/dT)_{max}/(1-X_{max}) = (E/nR) \cdot (1/T_{max}^2) \qquad (2.24)$$

The equation could be used to calculate the value of 'n', the order of reaction if value of activation energy 'E' is known. This equation is used in the present work to calculate the order of the reaction.

2.7 Thermal Conductivity / Diffusivity Measurement:

Thermal conductivity is an important property of a material to control heat transfer through it and other physical characteristics. The thermal storage capacity (ρ.Cp) in addition to its thermal conductivity influences the temperature distribution within a substance. So it is convenient to define the combination as thermal diffusivity

$$\alpha = (K / \rho.Cp.) \qquad (2.25)$$

Many methods are used to measure thermal conductivity and they vary in principle from simple steady state conduction[42] to recent laser flash method[43]. The selection of method depends on convenience and sample geometry.

Flash method for determination of thermal conductivity is one in which a sample in the form of a small disc is brought to a steady uniform temperature in a suitable furnace or cryostat. A flash of thermal energy is then supplied to the front surface of the sample within a short time interval. A very small sample could be used. Heating of the front face (x=0) is done by xenon lamp, electron beam or solid state laser. The energy absorption is maximized by blackening the exposed surface. Sensitive recording apparatus is used to give the temperature of rear face (x=L) as

function of time. Heat losses are minimised by making the measurements in short time.

According to Carslaw and Jaeger [44] for a sample which has a steady initial temperature distribution (T(x, 0) the temperature T (x,t) at any time 't' after receiving the flash at t=0, is given by,

$$T(x,t)=(1/L)\int_0^L T(x,0)dx+(2/L)\sum_{n=1}^{\infty}\exp(-n^2\pi^2\alpha t/L^2).\cos(n\pi x/L)\int_0^L T(x,0)\cos(n\pi x/L)\,dx \quad (2.26)$$

Assuming the pulse of energy 'Q' to be instantaneously and uniformly absorbed in a small depth 'g' at the surface 'x' (x=0) then at that instant the temperature distribution is

$$T(x,o) = Q / (d\,C\,g) \qquad \text{for} \quad 0 < x < g$$

$$T(x,0) = 0 \qquad \text{for} \quad g < x < L$$

For small value of 'g', the rear face temperature becomes,

$$T(L,t) = Q/dcL\left[1+2\sum_{n=1}^{\infty}(-1)^n\exp(-n\pi^2\alpha\, t/L^2)\right] \qquad (2.27)$$

The maximum rear face temperature will be

$$TL_{max} = Q/dcL$$

$$T(L,t)/T(L_{max}) = 1+2\sum_{n=1}^{\infty}(-1)^n\exp(-n^2\pi^2\alpha.t/L^2) \qquad (2.28)$$

When $T(L,t) / T(L_{max}) = (1/2)$,

The dimensionless quantity $\pi^2 \alpha t / L^2$ has a value of approximately 1.37 and then

$$\alpha = 1.37 L^2 / \pi^2 t_{1/2} = 0.139 L^2 / t_{1/2} \qquad (2.29)$$

Laser flash method is the recent and accepted method for measuring thermal conductivity. Figure 2.6 indicates the set up. Akiyama et al [10,14] and Kasai [32] used this method for iron ore and coke sample. In their method a pulsed ruby laser beam is flashed on the top surface of the disc specimen of 1 cm in diameter and 0.1 to 0.15cm thickness. Temperature response at the back surface of the sample is recorded by digital transient memory by Akiyama. Thermal diffusivity 'α' was calculated using equation:

$$D = 0.1388 A.L^2 / t_{1/2} \qquad (2.30)$$

where 'L' is the thickness of specimen, '$t_{1/2}$' is the specific time at which the back face temperature reached half of its maximum value, 'A' is the correction factors determined by the ratio of radiation loss. The measurement of thermal diffusivity was carried out in vacuum. The back surface of specimen was coated by spraying high emissivity carbon powder to improve the temperature response. Kasai, Murayama and Ono[32] used the same method for coke sample with different sample configuration. Platinum plate of very low thickness was welded on both side of the sample by platinum paste and the temperature response was noted by Pt -Pt 13%Rh thermocouple of 0.1 mm diameter. The sample configuration is shown in figure 2.7.

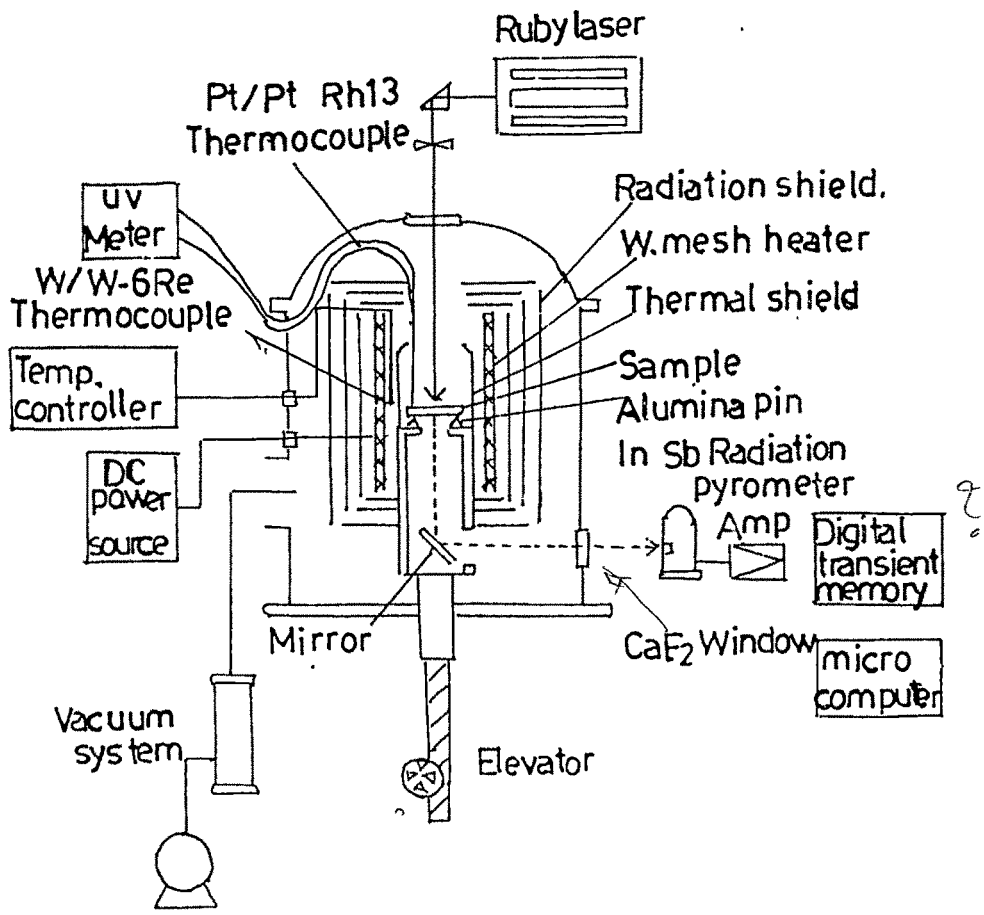

Fig. 2.6 Set-up of Laser flash method
(Ref No. 10 and 14)

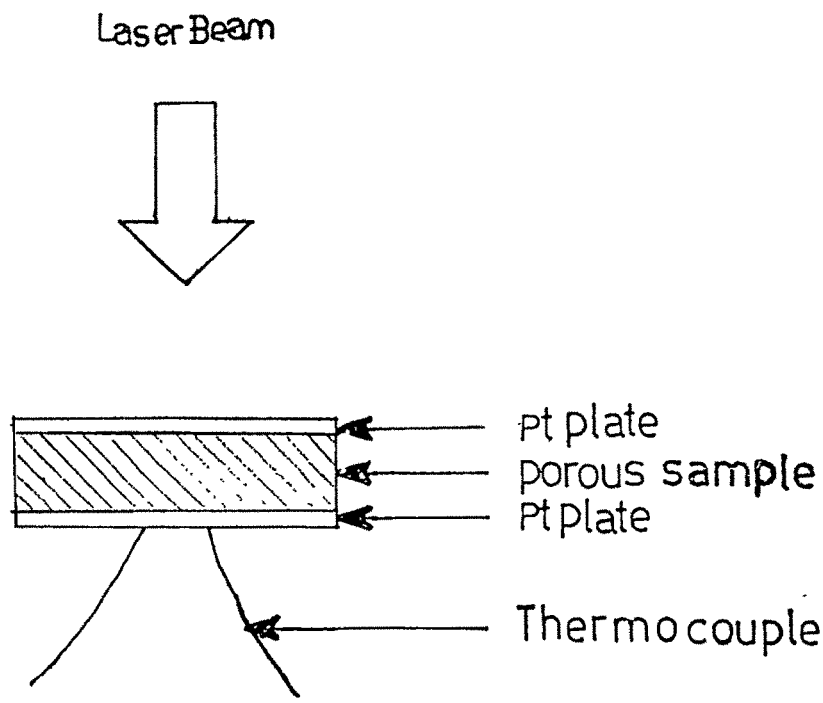

Fig. 2.7 Pellet configuration of Laser flash method (Ref. No.32)

The method is accurate specially to measure effect of temperature on thermal conductivity but its use is restricted to flat surface geometry and axial heat flow.

2.7.1 Radial heat flow method:

The thermal conductivity for radial heat transfer is reported in literature for cylindrical and spherical geometry. If the outer surface of a long cylindrical specimen of internal and external radius 'r_1' and 'r_2' is heated at a constant rate then the temperature difference T_2-T_1 established between the surface is

$$T_2 - T_1 = (1/2\alpha)\partial T/\partial t \; [(1/2)(r_2^2 - r_1^2) - r_1^2 \ln r_2/r_1] \quad \text{_____} \quad (2.31)$$

This equation assumes that the specimen is isotropic and homogeneous, with α independent of temperature.

Fitzsimmons described a method of measuring thermal diffusivity in which long cylinders are heated or quenched by rapid immersion in a well-stirred fluid and the subsequent temperature changes at the centre of the rod were observed. Equation 2.31 was the basis of method described by Flieger and Ginning with a difference that the two radii r_2 and r_1 at which temperatures are observed were located within the body of a hollow cylinder of inner radius r_0 . The appropriate equation becomes

$$\alpha = (1/2(T_2 - T_1))\partial T/\partial t \; [(1/2).(r_2^2 - r_1^2)) - r_0^2.\ln(r_2/r_1)] \quad \text{_____} \quad (2.32)$$

Abzalov and co-workers [45] determined the thermal conductivity of small cylinders of compressed magnetite concentrate over a range of temperatures and heating rates, their measurements were affected by the oxidation of magnetite and removal of combined water.

Recently Datta[46] used cylindrical geometry and different model equations to explain thermal and solidification behaviour of clay moulds and castings

The thermal conductivity measurement for spherical body for radial heat transfer is indicated by Wright, Watt and Vale.[47] They measured the temperature at centre and half radial distance of a pellet while heating and applied non isothermal heat transfer equations:

$$\partial T/\partial t = \alpha [\, \partial^2 T/\partial r^2 + (2/r)\,(\partial T/\partial r)\,] \qquad \text{(2.33)}$$

where ' T ' is temperature and ' t ' is the time, 'r' is the radial distance within pellets and 'α' is the thermal diffusivity.

The equation was solved for specific boundary condition. The experiments were conducted with dried and fired pellets. The temperature (Tr) at a radial distance 'r' at time 't' was assumed to follow.

In case of dried pellet[47]

$$Tr = a_0 + a_1 t + a_2 t^2 \qquad \text{(2.34)}$$

In case of fired pellet[48]

$$Tr = T\infty\,(1 - e^{-At}) \qquad \text{(2.35)}$$

The centre temperature 'Tc ' was corrected to To and T∞ by equations

$$Tc = T\infty(1 - e^{-At}) + 2T\infty \sum_{n=1}^{\infty} (-1)^n A/(n^2\phi - A)\,(e^{-At} - e^{-n^2\phi t}) \qquad \text{(2.36)}$$

where $\phi = \pi^2 \alpha / (R/2)^2$

The thermal diffusivity 'α' of a pellet was determined from the pellet temperature at r=0 and above equation with quasi-linearization technique. Thermal conductivity of the pellet was then calculated by the use of the average value of pellet density and the average value of heat capacity of the hematite pellets.

This pellet was hung in a closed refractory crucible and than placed in the hot zone. The refractory crucible reduced the non uniformity in the external heating of the pellet and decreases the initial rate of heating. The method used in present case is discussed in next chapter. . The method is based on Watts, Wright and Vale method with modifications. Since the values of thermal conductivities were measured on a pellet while heating, the range of temperature should be selected with care for minimum variation.

The variation of thermal diffusivity with temperature was studied by many investigators and summarized by Akiyama.[10] The result is reproduced here in figure 2.8. The results of Watt et al is also reproduced in figure 2.9. Both the figures

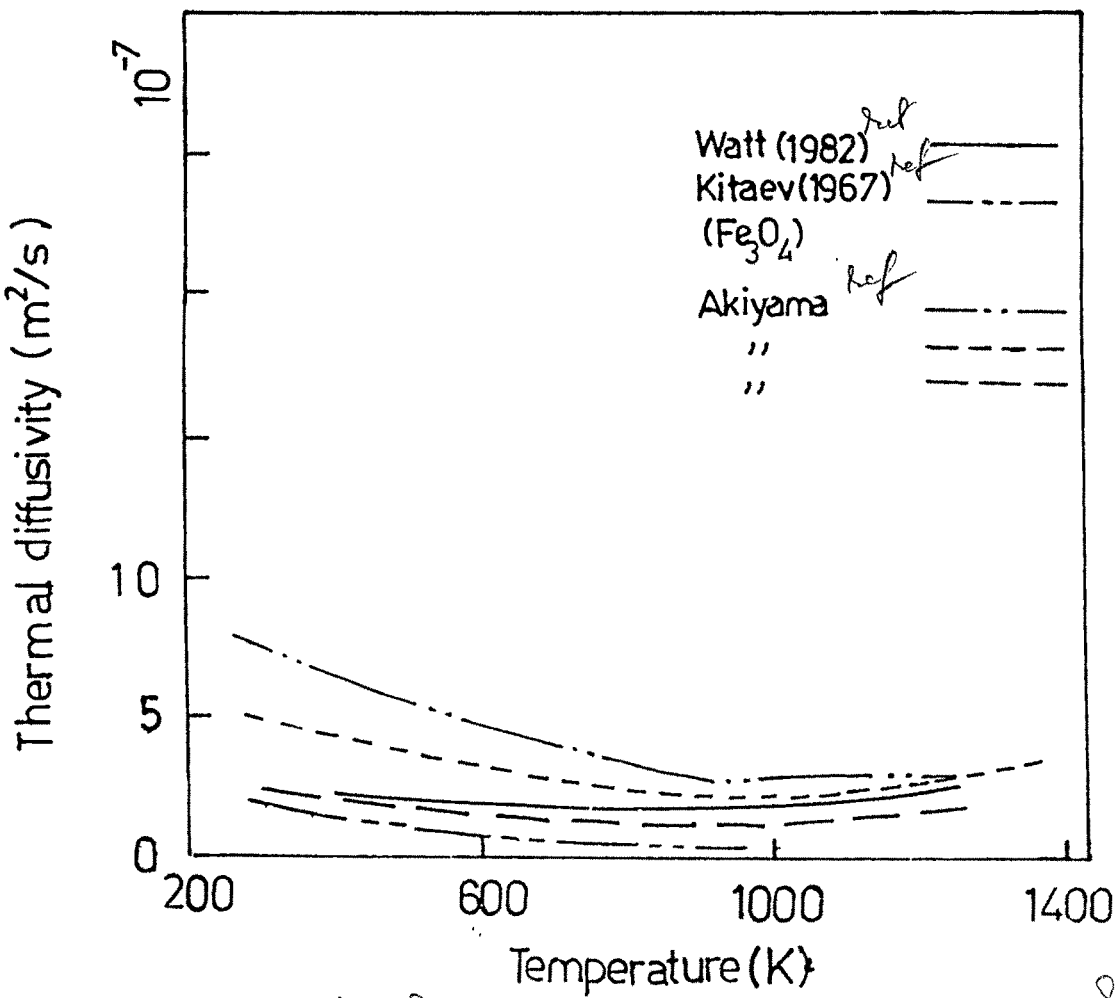

Fig. 2.8 Effect on thermal diffusivity of iron ores with temperature (Ref. No.14 and 10)

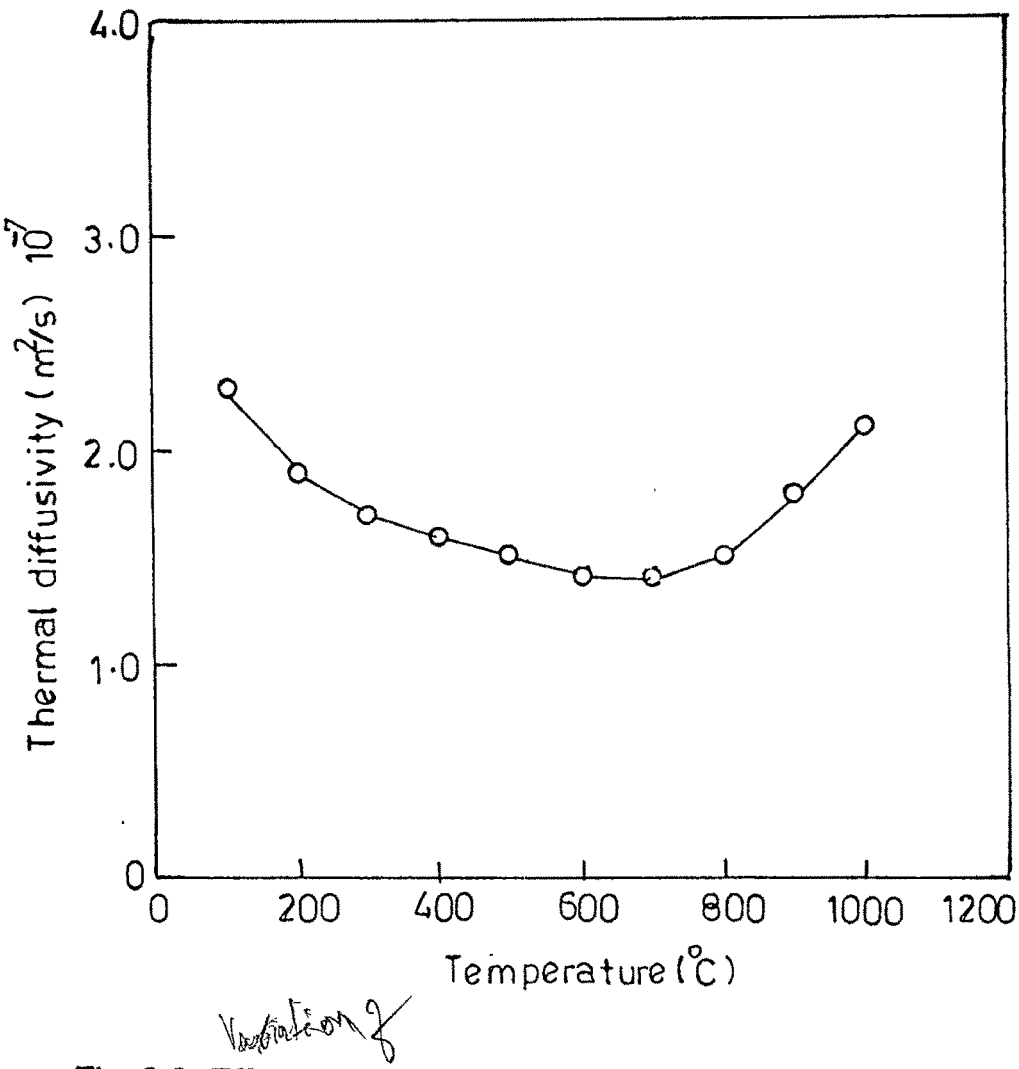

Fig. 2.9 Effect on thermal diffusivity of dried hematite pellet with temperature (Ref. No.48)

indicate that the variation in values of thermal diffusivity is negligible in temperature range of 400 - 800^{0}C.

2.7.2 Thermal Conductivity Vs Porosity

Akiyama and co-workers list many expressions available for co-relating thermal conductivity and porosity of a material. They explained their result by applying unit cell model suggested by Luikov [49]. The relations reported are

(a) $Ke = e\,Kg + (1-e)\,Ks$ _____ (2.37)

(b) $Ke = [\,e / kg + (1 - e)/ Ks\,]^{-1}$ _____ (2.38)

(c) $Ke = Ks^{1-e} . Kg^{e}$ _____ (2.39)

(d) $Ke / ks = (1- 2e\,(P-1) / (2P+1)) / ((1+ e\,(P-1) / (2P+1))$ [Eucken] _____ (2.40)

(e) $Ke / Ks = (e^{2/3} + P\,(1-e^{2/3})) / ((e^{2/3}- e + P\,(1- e^{2/3} + e))$ [Russel] ___ (2.41)

Where Ks: Thermal conductivity of pellet at zero porosity

Kg: Thermal conductivity of gas

P: Ks/Kg

Ke: Effective thermal conductivity.

e: Fractional porosity

These equations are derived by assuming different pore structures as cubic/spherical and neglecting the radiation within pores. Figure 2.10 indicate relationship between (Ke/Ks) Vs Porosity for different model equation.

Kunni's equation has been widely used for the estimation of effective thermal conductivity of porous media[10, 32]. The equation is given below.

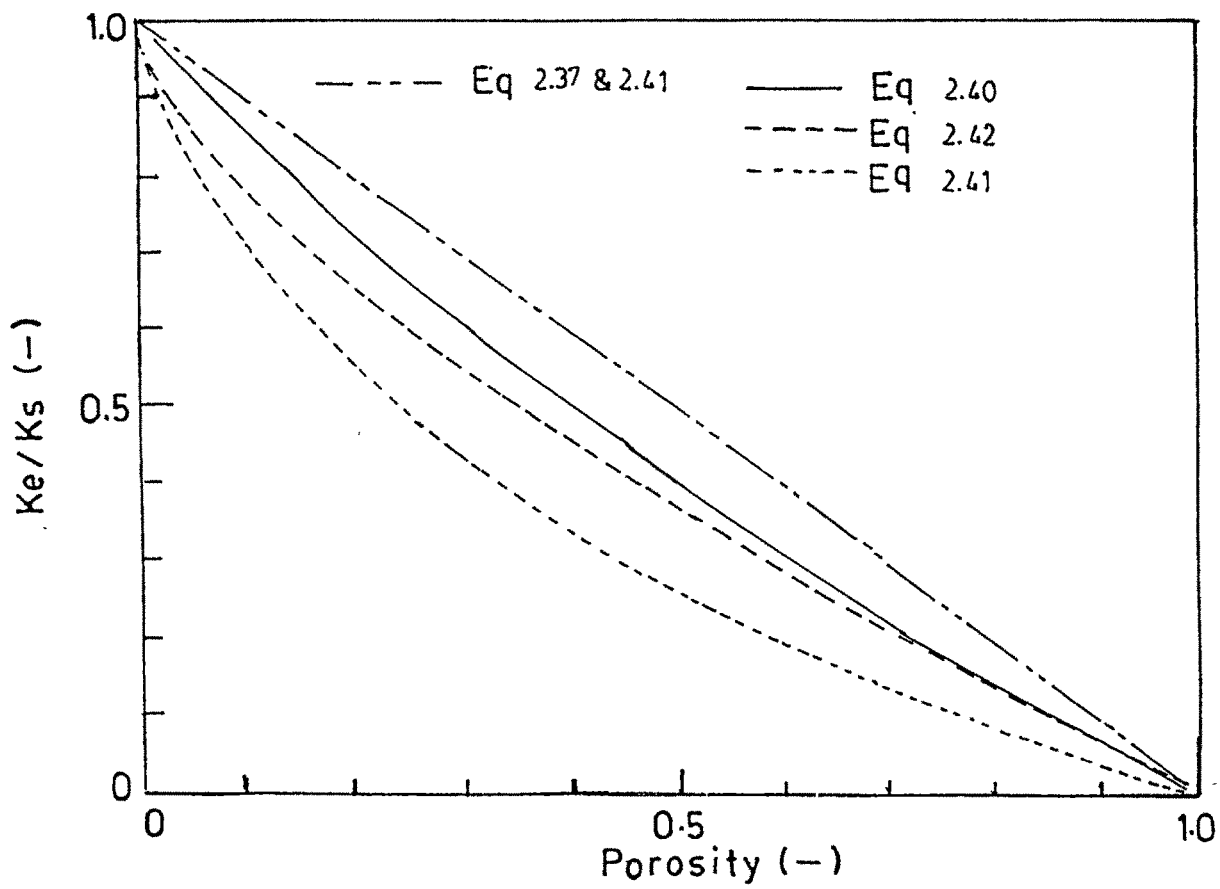

Fig. 2.10 (Ke/Ks) Vs Porosity for different model equation
(Ref. No. 10)

$$Ke/Ks = (1- e^{2/3}) + e^{2/3}[(1 - e^{1/3}) + e^{1/3} / \{(Kg / Ks) + (2/3)(h.d_p/ Ks)\}]^{-1} \quad (2.42)$$

Where 'h' is radiation heat transfer coefficient, 'e' is fraction porosity and 'dp' the pore diameter.

The right hand side of the equation is divided into two terms. The first term shows conductive heat transfer in the solid part and second term the contribution of rest.

The radiation heat transfer coefficient 'h' is also given by [32]

$$h= 0.2269 (\varepsilon/ 2-\varepsilon) (T/100)^3 \quad (2.43)$$

Where 'ε' is emissivity.

Nishioka, Murayama and Ono [50] observed that not only porosity but also pore size distribution has greater influence on thermal diffusivity. They also made an attempt to evaluate the contribution of radiative heat transfer within pores. Heat transfer between two gray surfaces by radiation is given by [51].

$$Q_{12} = \sigma \varphi_{12} (T_1^4 - T_2^4) \quad (2.44)$$

Where 'σ' is stefan Boltzmann constant and 'φ_{12}' is factor containing view factor and emissivity.

On the other hand, heat flux per unit surface per unit time is given as:

$$Q_{12} = - K\, dT/dx \qquad \text{(2.45)}$$

Apparent thermal conductivity of a pore for heat transferred by radiation was obtained by equating these two quantites.

$$-K\, dT/dx = -K\,(T_1 - T_2)/(X_1 - X_2) = \sigma\, \varphi_{12}\, (T_1^{\,4} - T_2^{\,4}) \qquad \text{(2.46)}$$

(X_1-X_2) is mean pore diameter d_p.

$$K = \sigma\, dp\, (T_1^{\,2} + T_2^{\,2})\, (T_1 + T_2)\, \varphi_{12} \qquad (2.47)$$

The above equation indicates that the apparent thermal conductivity of pore is proportional to the pore diameter. It could be calculated with assumption that the pore surface acts as a black body with a view factor '1'. Nishioka et al [50] calculated the contribution of radiation and found it to be negligible because thermal conductivity of solid part was 1000 times larger than apparent thermal conductivity of pore part at any temperature.

Nishioka [50] reported that two coke samples of equal porosity around 55-56 % but with average pore size of 109 μm and 208 μm has different thermal diffusivity values. Figure 2.11 indicates the microstructure of these samples. It could be seen that in sample 1, there are many micro-pores between macro-pores. Heat flow is intercepted in this case. In the second sample, there are fewer micro-pores and temperature decreases gradually.

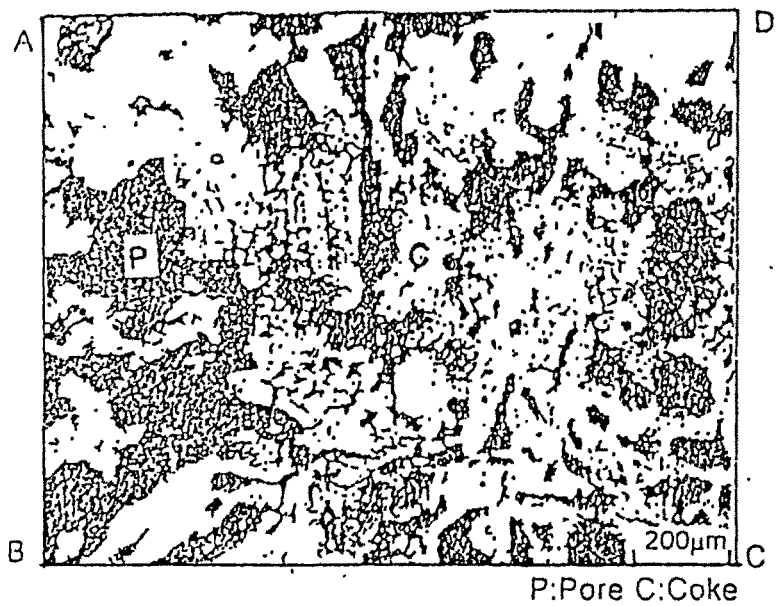

01

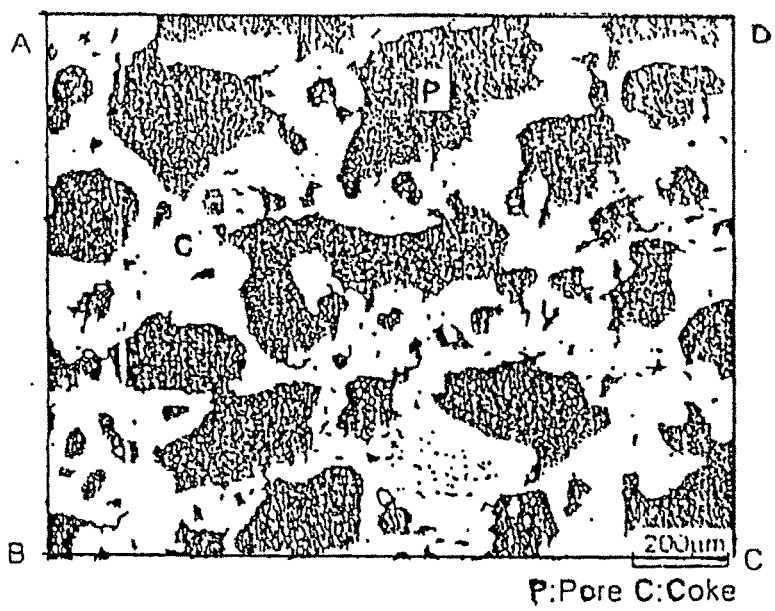

02

Fig. 2.11 Microphotograph of coke samples with same porosity but different average pore size(Ref No.50)

The calculation of thermal conductivity from thermal diffusivity requires the value of heat capacity of sample, which varies with temperature. The following table gives the values of true heat capacity of Fe_2O_3 with temperature [52].

Temperature (°C)	True heat capacity (kJ/kg.K)
0	0.615
100	0.724
200	0.799
300	0.854
400	0.904
500	0.955
600	1.000
700	1.047
800	1.093

The value of heat capacity at 700^0C is used in this work to calculate the thermal conductivity of iron ore pellets.